Guidelines of Creating Krylov-subspace Macromodels for Lateral Viscous Damping Effects

Po-Ching Yen and Yao-Joe Yang
Department of Mechanical Engineering
National Taiwan University, Taipei, Taiwan, ROC
TEL: +886-2-23646491 FAX: +886-2-23631755 E-mail: yjy@ccms.ntu.edu.tw

ABSTRACT

In this work, the guideline of generating *accurate* lateral viscous damping macromodels by the Krylov-subspace algorithm is described. A three-dimensional (3-D) finite-difference (FDM) Stokes flow solver for simulating lateral damping effects was developed. The system matrices generated by the solver was then reduced to low-order macromodels that can be easily inserted into a system-level modeling simulators, such as Saber, Simulink or SPICE for transient and frequency analysis. Based on physical and numerical constraints, the required orders of macromodels as well as the appropriate sizes of computational meshes are proposed. Finally, the experimental results for comb-drive devices show that the error of the results estimated by the macromodels are within 15%.

Keywords: lateral viscous damping, macromodel, model order reduction, comb-drive, system-level analysis

INTRODUCTION

Many MEMS devices such as accelerometers, gyroscopes, switches, micro-mirrors, and resonant sensors need fully understanding of lateral gas damping effects for accurate dynamic modeling. It is well known that modeling 3-D lateral viscous damping effects using FEM or FDM not only requires intensive solid-modeling work, but also require significant computational resources even for a steady incompressible-flow simulation. Therefore, earlier works on lateral viscous damping were based on the 1-D analytical Stokes and Couette flow solutions [1,2]. The 1-D analytical approaches can easily provide the first-order estimation of lateral damping effect, and require almost negligible computational resources so that they are intrinsically compatible with any system-level simulators. However, the 1-D approaches over-simplify the geometrical complexity of typical MEMS devices with lateral damping effects, and thus the error is very large in most cases.

Recently, Aluru and Wang [3,4] developed 3-D Stokes solvers using boundary-element method (BEM), and demonstrated that the BEM approaches not only require much less computational cost than typical FEM/FDM approaches [5], but also significantly reduce the works on creating solid models. However, the solutions of the BEM approaches are in frequency domain, and hence are not completely compatible with transient analysis. In this work, we develop model-order-reduction (MOR) methodology [6,7,8,9] for generating accurate *time-domain* macromodels from 3-D FDM/FEM Stokes solvers, and explore the characteristics of the macromodels under various conditions.

Figure 1 outlines the concept of the model-order-reduction procedure for lateral damping effects. The initial step of generating the macromodels is to generate 3D solid models. This step is very similar to the typical procedure of performing FEM//FDM fluidic simulation. However, we used the commercially-available MEMS modeling packages, such as Coventorware, IntelliSuite and MEMS-Pro, to generate the 3D solid model of the air film from 2-D mask layout, by considering the air-film surrounding the structures as the fictitious sacrificial layer. After creating the solid model of the air film surrounding a MEMS laterally-movable structure, the FEM/FDM techniques are used to discretize the solid model. Since the governing equation is in time domain, the discretization creates a system (set) of ordinary differential equations whose state variables are in fact the velocity distribution of the air film. Typically the system is so large that huge computational resources for time-domain integration are required. Without direct integration of the system, the Arnoldi algorithm is applied to reduce the system of differential equations into a low-order system, the so-called macromodel. The macromodel can be readily inserted into system-level simulators, such as Saber® or Simulink®, for transient and frequency-response analysis.

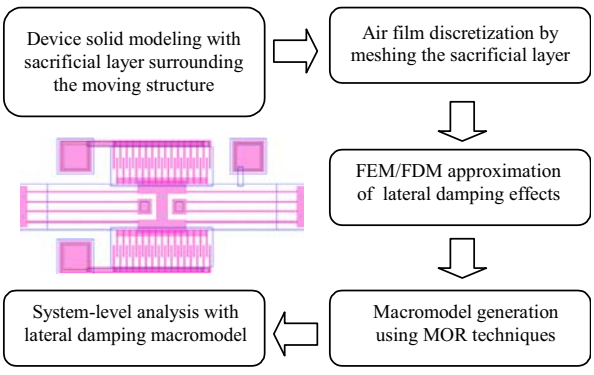

Figure 1: *Procedure of extracting lateral damping macro-model for MEMS devices*

In the following section, the theory of the fluidic damping effects and the application of the model-order-reduction technique are presented. Based on physical and numerical constraints, the required orders of macromodels as well as the appropriate sizes of computational meshes are proposed. Finally, the measured and simulated results are demonstrated.

THEORY

The governing equation of lateral viscous damping is the Stokes equation. The 3-D Stokes' equation is:

$$\rho \frac{D\vec{V}}{Dt} = -\nabla p + \mu \nabla^2 \vec{V} \quad (1)$$

where p is pressure, ρ is the density of the gas, μ is the viscosity coefficient, and $\vec{V} = \begin{bmatrix} u & v & w \end{bmatrix}^T$ is the velocity vector. For our case, the imposed pressure gradient is assumed to be zero, so the first term on the right-hand side can be eliminated. Since the damping contributed by the surfaces, whose normal vectors are parallel to the direction of plate motion, is negligible under our assumptions of $u >> v \approx w$, the velocity components perpendicular to the direction of the in-plane motion are ignored. As a result, the continuity equation is not considered [1], and Equation (1) can be simplified to:

$$\frac{\partial u}{\partial t} = \upsilon \nabla^2 \mu = \upsilon \left(\frac{\partial^2 u}{\partial x^2} + \frac{\partial^2 u}{\partial y^2} + \frac{\partial^2 u}{\partial z^2} \right) \quad (2)$$

where $\upsilon = \mu / \rho$ is the kinetic viscosity. Based on this equation, a finite-difference solver is developed.

Furthermore, the simplified governing equation, as shown in Equation (2), is a linear equation, so the system matrices generated by the FDM approximation process can be reduced by an Arnoldi-based model-order-reduction (MOR) technique. The dynamic system equation formulated by the FDM approximation of Equation (2) can be written as:

$$\begin{aligned} \dot{\vec{u}} &= \mathbf{A} \cdot \vec{u} + \mathbf{B} \cdot v_{in} \\ \vec{y} &= \mathbf{C}^T \cdot \vec{u} + \mathbf{D} \cdot v_{in} \end{aligned} \quad (3)$$

where $\mathbf{A}$ is an n by n matrix and n is the total number of nodes, $\vec{u}$ is the vector which contains the unknown velocity distribution on each node, and the input function v_{in} is the imposed velocity on the moving boundary of the computational domain. In this case, we carefully formulate $\mathbf{C}$ and $\mathbf{D}$, so that the output $\vec{y}$ will be the frictional shear (calculated by Newtonian law of viscosity) on the plate. In Laplace domain, the transfer function of the system is:

$$\begin{aligned} T(s) &= \mathbf{C}^T (\mathbf{I}s - \mathbf{A})^{-1} \mathbf{B} + \mathbf{D} = \mathbf{C}^T (\mathbf{I} - s\mathbf{A}^{-1})^{-1} \vec{b} + \mathbf{D} \\ \vec{b} &= -\mathbf{A}^{-1}\mathbf{B} \end{aligned} \quad (4)$$

After expanding the transfer function in Taylor series about *s=0*, we obtain:

$$T(s) = \mathbf{C}^T (\mathbf{I} + s\mathbf{A}^{-1} + s^2\mathbf{A}^{-2} + \ldots)\vec{b} + \mathbf{D} = \sum_{k=0}^{\infty} m_k s^k + \mathbf{D} \quad (5)$$

where m_k are the coefficients of the Taylor series, and are equal to $m_k = \mathbf{C}^T \left(\mathbf{A}^{-k} \right) \vec{b}$.

The Taylor expansion can be truncated to approximate the transfer function $T(s)$. Since $\mathbf{A}^{-k}\vec{b}$ quickly line up with a single eigenvector, this moment matching procedure is usually numerically unstable. Therefore, we apply the Arnoldi-based algorithm to stably compute orthogonal bases v_i that spans the Krylov subspace:

$$K_q \left(\mathbf{A}^{-1}, \vec{b} \right) = span\left\{ \vec{b}, \mathbf{A}^{-1}\vec{b}, \mathbf{A}^{-2}\vec{b}, \cdots, \mathbf{A}^{-(q-1)}\vec{b} \right\} \quad (6)$$

Given the matrix $\mathbf{V_q}$ whose columns are $\{v_i\}$, the Arnoldi algorithm reduces the system matrix $\mathbf{A}$ to a small upper Hessenberg matrix $\mathbf{H_q}$ whose entries are the Gramm-Schmidt orthogonalization coefficients:

$$\mathbf{V_q}^{\mathbf{T}} \mathbf{A} \mathbf{V_q} = \mathbf{H_q} \quad (7)$$

Finally, the reduced transfer function can be written as:

$$T_q(s) = \mathbf{C}^T \mathbf{V_q} \left(\mathbf{I_q} - s\mathbf{H_q} \right)^{-1} \mathbf{V_q}^T \vec{b} + \mathbf{D} \quad (8)$$

Note that the reduced system transfer function, as shown in Equation (8), has the same input (v_{in}) and output ($\vec{y}$) as those in Equation (3). Since the typical sizes of the system matrices are very small, the computational efficiency for simulating transient responses and frequency responses of the reduced models are significantly increased [7].

COMB-DRIVE DEVICE SIMULATION

The picture of the simulated and measured comb-drive structure fabricated by MUMPs® process is shown in Figure 2. A DC biase of up to 70 V and a sinusoidal driving voltage with amplitude (peak to peak) up to 20 V are used. The lateral fluid damping effect surrounding the comb drive is simulated and then compared with the experimental results to verify the accuracy of the developed 3-D Stokes solver.

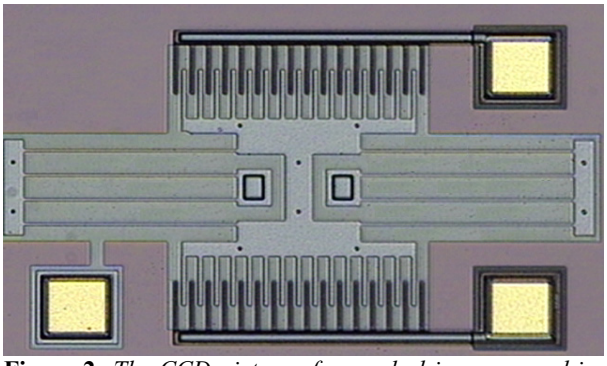

Figure 2: *The CCD picture of a comb-drive measured in this work*

I. Study on Discretization Convergence

Figure 3 shows the schematic of velocity profiles induced by a laterally oscillating plate for different frequencies. Figure 3(a) shows that when the structure oscillates at relatively low frequency, the air film above the structure is assumed to be of Stokes-type, and the air film underneath the structure is assumed to be of Couette-type. As the oscillating frequency increases (as

shown in Figure 3(b)), the velocity profiles will extend only to a short distance from the structure surface (i,e. short penetration depth of the velocity profile). In this case, even for small-amplitude motion, the air film will introduce a considerable amount of damping [1].

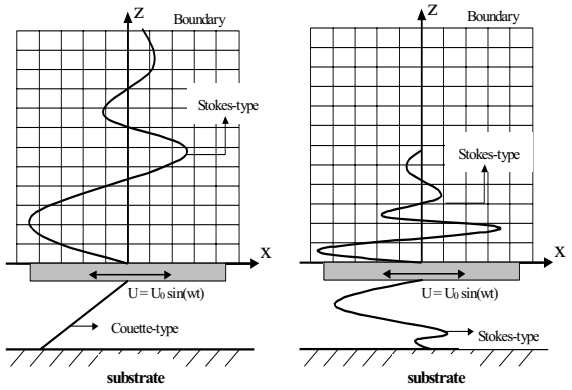

Figure 3: *Velocity profiles induced by a laterally oscillating structure with (a). low frequency, (b). high frequency.*

Therefore, under higher oscillating frequency, finer discretization of the FDM calculation in z-direction is required because the spatial variance of the Stokes-flow's velocity profiles is much higher than the counterpart of the Couette-type flow. Figure 4 shows that the required maximum discretization length in z-direction is about 0.2 μm for simulating converged shear force results at frequency below 1 MHz. In other words, if the operating frequency is higher than 1 MHz, the discretization length has to be less than 0.2 μm since the penetration depth of the velocity profile decreases.

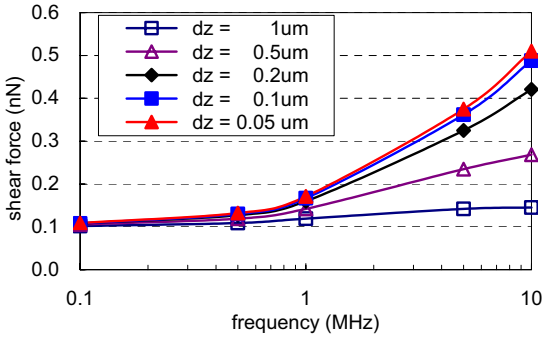

Figure 4: *The total shear force vs. oscillating frequency for a comb structure. The simulation accuracy for high frequency model (>1 MHz) is strongly relative to the distance between the meshing nodes.*

II. Required Extent of Fluidic Domain

Figure 5 shows the relationship between the upper air film thickness and the simulated shear force of the device. When oscillating at a frequency higher than 1MHz, the shear forces calculated by the FDM/FEM models with different upper air-film thickness are the same. However, as the frequency decreases, the model with thin computational domain overestimates the damping, since the assumption of zero-velocity boundary on the top of the air film is no longer valid. This figure also indicates that the minimum air-film thickness is about 10 μm for a frequency as low as 10 kHz.

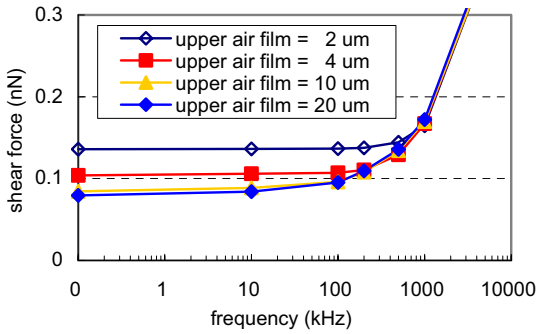

Figure 5: *Shear force versus oscillating frequency for different air film thickness above the moving structure.*

The shear forces contributed by different parts of the air film are shown in Figure 6. The damping contributed by the underneath film increases as the oscillating frequency increases, and finally becomes comparable to the damping contributed by the top film when the frequency is higher than 500 kHz.

Figure 7 is the frequency response of the system damping shear force for different order macromodels, and indicates that the macromodels with orders greater than 15 are required for the converged results under a wide range of operating frequencies (from 10 kHz to 10 GHz).

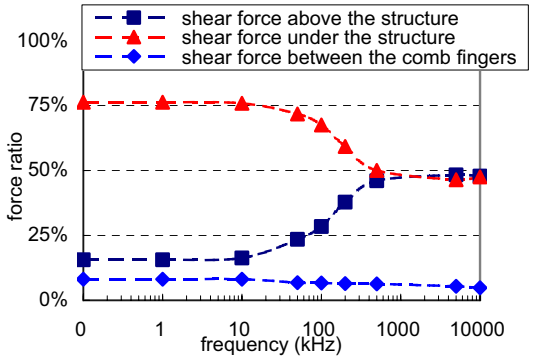

Figure 6: *The contribution of the shear force ratios by the air film above the structure, under the structure and between the comb fingers.*

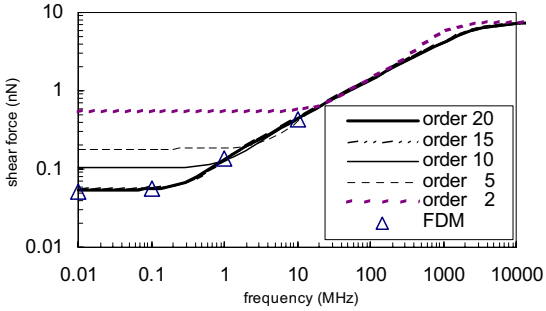

Figure 7: *Shear force versus frequency for the macromodels with different orders.*

SYSTEM-LEVEL SIMULATION COMPARED WITH MEASUREMENT

The macromodels generated by the Arnoldi-based MOR algorithm can be readily inserted into system-level simulators, such as Saber® or Simulink®, for transient and frequency-response analysis. Figure 8 presents the experimental results of the comb drive device with folded beam length of 228 μm as well as the system simulation results of the 20th order damping macromodel. The macromodel underestimates the damping by about 10% in this case, and we speculate the major source of this error comes from the fact that the macromodel neglects the pressure back force on the tip-ends of the comb figures. Figure 8 shows the simulated and measured comb-drives quality factors vs. different folded-beam lengths. The results by the 1-D Stokes/Couette analytical models are also presented in the Figure. The 1-D analytical model over-predicts the quality factors by 30~40%, while the discrepancy between the measured results and the macromodels is within 15%.

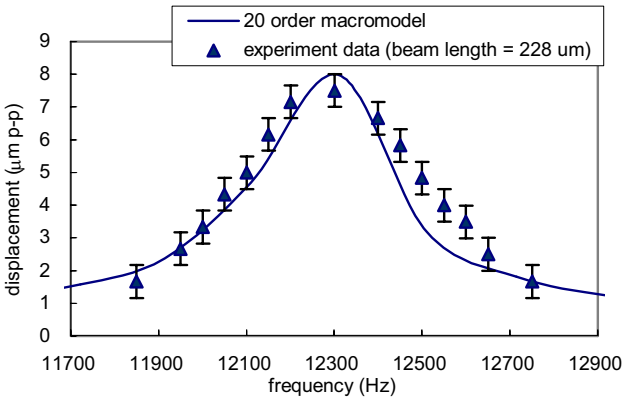

Figure 8: *Frequency response of the 20 order macromodel of the comb drive device with 228 μm folded beam compared with the experimental data.*

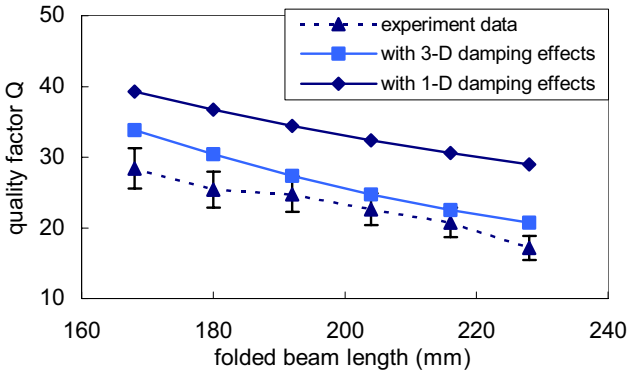

Figure 9: *Comb-drive quality factors vs. different folded-beam lengths are shown.*

CONCLUTION

This paper presented a 3-D FDM Stokes' solver, and a macro-model generation methodology for lateral damping effects based on the application of Arnoldi-based model-reduction technique. The theory of the Arnoldi-based model-order-reduction is described. The studies on the FEM/FDM mesh convergence and the appropriate size of computational domain were also discussed. The macromodels generated by the technique were successfully inserted into the Simulink for system level analysis, and the results were also compared with the experimental data. The discrepancy of the simulated and measured quality factors are within 15%.

Acknowledgement

This research was supported by the National Science Council (Grant No. 91-2218-E-002-021), Taiwan, R.O.C.

REFERENCES

1. Y.-H. Cho, A. P. Pisano and R. T. Howe, "Viscous damping model for laterally oscillating microstructures," *J. Microelectromechanical Systems*, Vol. 3, No. 2, Jun. 1994, pp. 81-87.
2. T. Veijola and M. Turowski, "Compact damping models for laterally moving microstructures with gas rarefaction effects," *J. Microelectromechanical Systems*, Vol. 10, No. 2, Jun. 2001, pp. 263-273.
3. N. R. Aluru and J. White, "A fast integral equation technique for analysis of microflow sensors based on drag force calculations," in *Proc. of MSM*, Santa Clara, USA, Apr. 1998, pp. 283-286.
4. X. Wang, M. Judy, and J. White, "Validating fast simulation of air damping in micromachined devices," in *Proc. IEEE 15th International Conference on Micro Electro-mechanical Systems Workshop (MEMS 2001)*, Las Vegas, USA , Jan. 2002, pp. 210-213.
5. W. Ye, X. Wang, W. Hemmert, D. Freeman, and J. White, "Viscous drag on a lateral micro-resonator: fast 3-d fluid simulation and measured data," in *Tech. Dig. of 2000 Solid-State Sensor and Actuator Workshop*, Hilton Head Island, SC, Jun. 2000, pp 124-127.
6. P.-C. Yen and Y.-J. Yang, "Time-domain reduced-order models of lateral viscous damping effects for 3d geometries," in *Proc. of MSM,* 2002, San Juan, Puerto Rico, USA, Apr. 2002, pp. 190-193.
7. P.-C. Yen and Y.-J. Yang, "Macromodels of 3d lateral viscous damping effects for mems devices", *in* Proc. 12th International Conference on Solid-State Sensors and Actuators (Transducers '03)*, Boston, USA, June, 2003, pp. 1848-1851.*
8. Y.-J. Yang, M. Kamon, V. L. Rabinovich, C. Ghaddar, M. Deshpande, K. Greiner and J. R. Gilbert, "Modeling gas damping and spring phenomena In mems with frequency dependent macromodels," in *Proc. IEEE 14th International Conference on Micro Electro-mechanical Systems Workshop (MEMS 2001), Interlaken, Switzerland, January 2001, pp. 365-368.*
9. A. Odabasioglu, M. Celik, and L. T. Pileggi, "PRIMA: passive reduced-order interconnect macro-modeling algorithm," in *Proc. IEEE Transaction on Computer-Aided Design of Integrated Circuits and Systems,* Vol. 17, No. 8, Aug. 1998, pp. 645-654.
10. J. A. Fay, Introduction to Fluid Mechanics, MIT Press, Cambridge, 1994.